3D Multi-Agent Models for Protein Release from PLGA Spherical Particles with Complex Inner Morphologies

Ana Barat,[1] Heather J. Ruskin[2] and Martin Crane[3]

[1] Dublin City University, Dublin 9, Ireland, Tel. +353 1 700 5669,
   `abarat@computing.dcu.ie`
[2] Dublin City University, Dublin 9, Ireland, Tel. +353 1 700 5000,
   `hruskin@computing.dcu.ie`
[3] Dublin City University, Dublin 9, Ireland, Tel. +353 1 700 8974,
   `mcrane@computing.dcu.ie`

Abstract: In order to better understand and predict the release of proteins from bioerodible micro- or nanospheres, it is important to know the influences of different initial factors on the release mechanisms. Often though it is difficult to assess what exactly is at the origin of a certain dissolution profile. We propose here a new class of fine-grained multi-agent models built to incorporate increasing complexity, permitting the exploration of the role of different parameters, especially that of the internal morphology of the spheres, in the exhibited release profile. This approach, based on Monte-Carlo (MC) and Cellular Automata (CA) techniques, has permitted the testing of various assumptions and hypotheses about several experimental systems of nanospheres encapsulating proteins. Results have confirmed that this modelling approach has increased the resolution over the complexity involved, opening promising perspectives for future developments, especially complementing *in vitro* experimentation.

Keywords: drug delivery, drug release, PLGA, protein, microspheres, nanospheres, modelling, simulation, Monte Carlo, Cellular Automata.

1 Introduction

In this paper, a range of multi-agent models for simulating dissolution of macromolecules from bioerodible spheres is introduced. Bioerodible micro- and nanospheres, encapsulating large molecules such as proteins, have been at the cutting-edge of development in the area of novel drug delivery systems

for sustained release, with applications in bioengineering fields including bone repair, tissue engineering and development [3, 21, 6], as well as in biomedical areas such as vaccine delivery, various chemotherapies for treatments of cancer, AIDS, tuberculosis, diseases of the central nervous system [5, 20, 12, 4] and others. Interest in using biodegradable materials lies in the fact that the products of dissolution of the particles are biocompatible and biodegradable, hence they do not require further manipulation after introduction to the body [21]. This makes bioerodible particulates suitable for use under minimum invasive surgery [16], providing greater patient compliance.

In particular, the present paper focuses on drug delivery systems using poly(lactide-co-glycolide) (PLGA) as a bioerodible material to encapsulate proteins and other large molecules. This non-toxic, biodegradable material is widely used in the controlled-release community, because its physical and chemical properties permit the manufacture of a large spectrum of micro- and nanoparticles, generating various release profiles for the encapsulated drug. Recent work [18, 15] has also indicated that these drug carriers exhibit extremely complex dissolution behaviour. Experimentation *in vitro* is both costly and time-consuming: the release period for a PLGA particle can range from 3 weeks to 1 year [21], hence an increased interest for complementary modelling and simulations.

In silico modelling of dissolution from PLGA spheres has proved to be a very laborious task in the reduction and replacement of such *in vitro* experimentation. PLGA is a bulk-eroding material so erosion takes place slower than the hydration of the particles. As a result, the erosion occurs through the entire volume of the spheres, creating a network of pores and channels through which the encapsulated molecules escape the delivery system, so the

modelled system is non-homogeneous. Figure 1 illustrates the principle of bulk erosion compared to the more common process of surface erosion.
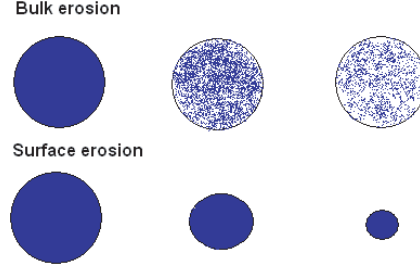
Fig. 1. Bulk erosion versus surface erosion.

In the dissolution of PLGA spheres, we can distinguish two simultaneous processes which need to be modelled: i) *the erosion of the polymer* and ii) *the dissolution of the encapsulated molecule*. An approach, recently gaining popularity in modelling polymer erosion, is based on direct MC and CA methods. In the case of bioerodible polymers, the work of Göpferich [7, 9, 6, 8] and Zygourakis [25] has shown that polymers, their properties and the process of their dissolution can be modelled microscopically by means of computational grids with transient behaviour. The eventual release of an encapsulated drug is considered to be directly proportional to the erosion of polymer [9, 8]. This approach, usually based on the assumption that the polymer has a homogeneous inner structure, aims for a good representation of the geometrical form of the devices, as well as of the physical and chemical interactions inside the matrix, and has led to promising results and potential for further development.

A range of models, based on numerical solutions of differential equations, focusing more on the second process, (the dissolution of the encapsulated molecule), simulates the concentrations of diffusing species within and external to the spheres [2, 10, 19, 23]. Methods based on differential equations require,

for example, continuous spatial distributions, hence they consider porous 3D morphologies indirectly, in introducing porosity parameters that affect the diffusion coefficients through time and space [23, 10, 19]. In [10, 19], previous work involving microscopic models based on MC was used in order to calculate the porosity parameters needed to solve the differential equations.

To date 1) there are no reports using fine-grained models to analyse the effects of the internal morphologies of PLGA spheres on the dissolution profiles and 2) there are no microscopic models *directly* taking into consideration the dissolution of proteins from PLGA devices. However, recently published, parallel work has shown the interest of the researchers in developing more sophisticated microscopic models for polymeric applications in drug delivery. For example, the proteins are viewed as distinct entities in a very interesting microscopic model for the release of proteins from cross-linked dextran microspheres [22].

In the present study, PLGA drug carriers were represented as complex 3D systems, departing from the idea that, in addition to the factors already considered in the cited literature, in the case of protein dissolution, both the *pre-existent* and *dynamically formed* pores influence in a direct way the resulting protein release profile. This work examines, in a very fine-grained manner, the 3D internal morphologies of nanospheres, using MC agent-based models to explicitly simulate not only the erosion of the PLGA, but also the dissolution of the proteins themselves. The models were tested on experimental data from Sandor et al. [18], demonstrating very good performance. This work completes and also complements previous work done on probabilistic microscopic modelling of drug dissolution, demonstrating new possibilities of the multi-agent computational modelling techniques in a concrete example.

2 Theory

In the case of PLGA spheres, the range of factors responsible for variations in the dissolution profiles generated and/or inter-relationships of interacting factors is wide, and those with a crucial impact on the final dissolution profile are not straightforward to separate, [18]. However several general points may be made:

- In general, the drug release rate from PLGA spheres is controlled by the degradation rate of the PLGA co-polymer [11, 21, 2]. Selecting adequate formulation conditions, such as polymer type and preparation method, can generally regulate degradation rate. For example, the use of copolymers of PLGA of different molecular weight, hydrophilicity and copolymer composition (the ratio of lactide to glycolide) has been found to change initial hydration and erosion rate for the matrix [11, 21].

- The structure of the porous environment in the spheres also governs the protein release rate, (see Figure 2). The sphere processing parameters and copolymer composition is known to influence the extent of crystallinity and therefore the ratio of smaller to larger pores in the sphere [2]. The method of sphere preparation and molecule encapsulation plays a basic role in regulating the porosity factor. The type of encapsulated protein also has considerable influence on the inner morphology [18].

- In addition, drug diffusion in the pores influences the overall drug release profile and is conditioned by a group of factors such as molecular properties (hydrophilicity, size) and drug distribution (size distribution of the encapsulated powder particles and distribution of this powder inside the sphere, Figure 2).
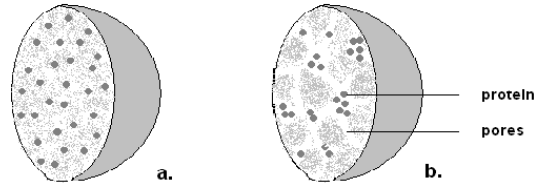
Fig. 2. a) Sphere morphology obtained by the solid-in-oil-in-water solvent evaporation technique [21]. b) Sphere morphology obtained by water- in-oil-in-water [21] solvent evaporation technique. Adapted from Ungaro et al. [21].

It is more difficult to modify the release characteristics of the spheres, once a polymer type and a preparation technique have been selected [21]. In this case, control over the release rate may be maintained either by modifying the internal morphology of the system (the porosity pattern) or adding a third component that alters drug effective diffusivity in the polymeric matrix [21].

A wide range of dissolution profiles can be generated by using PLGA spheres, but the most typical profile, with its three dissolution phases, (described in [2]), is given in Figure 3.
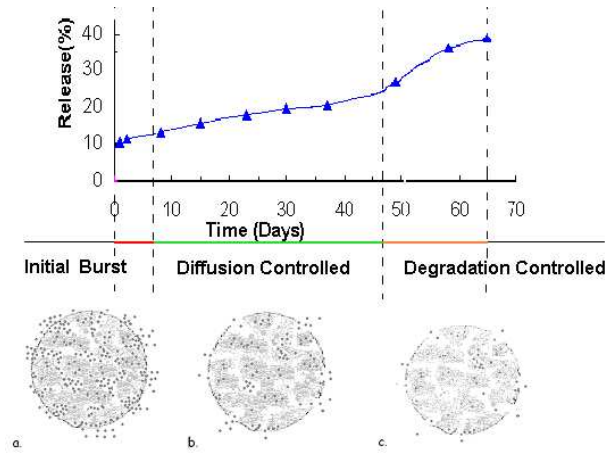
Fig. 3. Phases of protein release from PLGA microspheres, differing by shape of the curve and by dissolution mechanism: a) initial burst related to desorption or dissolution. b) erosion and diffusion. c) mostly erosion and diffusion.

The combination of parameters mentioned and the initial morphology of the sphere determine existence and duration of phases.

3 Modelling

The dimensions of the experimental entities involved range from several nanometers (proteins) to several microns (spheres). A comparatively simple protein example like the lysozyme (13.4 kDa), has a diameter of 3.2 nm [13]. Diffusion measurements in PLGA micro- and nanospheres encapsulating lysozymes involve pore sizes < 20 nm [18], so it is reasonable to describe diffusion in terms of individual random walks of molecules, rather than by transport of matter through surfaces. Experimental studies [18], have revealed that, in general, the initial configuration of pores corresponds mostly to sizes of 5 - 80 nm, (proportional to the size of the encapsulated proteins). Equally, other experimental studies have reported cases of spheres with *initial occlusions* much larger than the Stokes-Einstein diameter of the microencapsulated molecule [2, 3]. Nevertheless, as long as the proteins undergo very restricted diffusion through pores of i) the same order of magnitude as the proteins themselves or ii) slightly larger, but where other secondary phenomena, not specifically modelled here, form obstacles [4], it is appropriate to treat diffusion by individual random walks of a given number of agents [14, 17]. In such cases, multi-agent systems seem reasonable approximations for a "protein - PLGA - pore" system.

---

[4] Sometimes the drug has to move through some narrow passageways which are produced by the vibrations of the polymer chain and control the actual size for the passage of macromolecules, [23].

3.1 Main Characteristics of the Model

The assumptions which apply to all models developed are based on available experimental data [18]. The polymeric particles, modelled in 3D space, are considered to be completely spherical. The spheres are discretised throughout the volume into small sites. Figure 4 represents a schematic diagram of a section through a sphere during the simulation. The sites are seeded, according to predefined initial patterns, with elements such as PLGA polymer or protein molecules. If necessary, an initial porosity value in the PLGA bulk material can be considered and, over time, more pores are formed. Different strategies for describing PLGA erosion and pore formation can be considered. The approach taken here to model the polymer erosion was based on Göpferich's theory for polymer erosion [9]. When a site, filled with polymer, reaches a certain stage of erosion (the value of its lifetime reaches zero [9]), its status changes to that of a pore. A protein molecule can leave its initial location only in the case where one of the neighbouring sites is a pore, (i.e. the molecules can only move through pores). Once in a porous channel, a molecule cannot leave it, except by escaping the sphere. When a molecule escapes the sphere, it is counted as dissolved. The internal configuration of the spheres in the model can be varied, depending on the internal morphology of the experimental spheres. The algorithm used to perform the simulation can be resumed in the following:

1. Generate the nanosphere and populate it with the agents.
2. Update the state of the PLGA sites.
3. Update the state of the molecules: they can move or not to a neighboring pore.
4. Update the time and return to point 2.
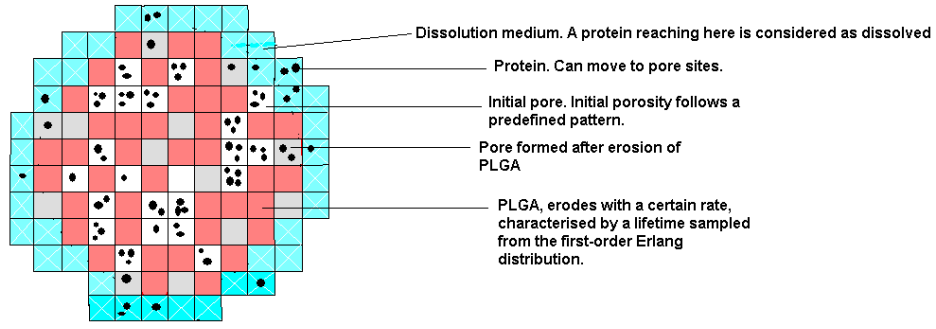
Fig. 4. Simplified scheme representing the main characteristics of the multi-agent model. Cross section through a 3D sphere.

## 3.2 Modelling the internal configuration of the spheres

The majority of modelling approaches available such as [23, 9] were designed for homogeneous distributions of the pores and of proteins in the spheres. Different aspects, suggesting that, in some cases, the internal configuration of the spheres might be subject to heterogeneity, are presented here.

The study conducted by Sandor et al. [18] on the effect of microencapsulated molecules on the internal structure of and nanospheres, revealed that spheres enclosing smaller proteins appear to have an open branched network throughout. However, those enclosing larger proteins have pores in the outer layers and appear open near the surface, while having a more dense structure in the inner layers of the sphere, Figure 5.
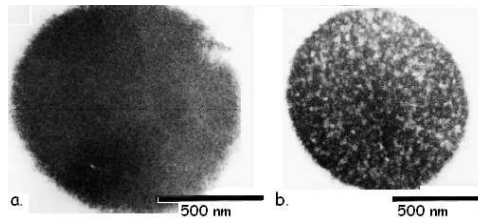
Fig. 5. a) Control PLGA sphere, no encapsulated molecules b) PLGA sphere encapsulating carbonic anhydrase, adapted from Sandor et al. [18].

Batycky et al. [2] discussed another phenomenon of relevance to microspheres. If it is assumed that adsorption of macromolecules to the surface of the microsphere (or to the large occlusions inside the spheres), an uneven distribution of the macromolecule throughout the sphere volume may occur. A recent 3D reconstruction from transmission electron microscopy (TEM) images of the transient distribution of albumin in PLGA spheres during erosion [24] shows an inhomogeneous distribution of the protein. If this uneven distribution is realistic, the values of parameters, obtained by adjusting models premised on a homogeneous distribution to experimental data (like in [23]), will be biased.
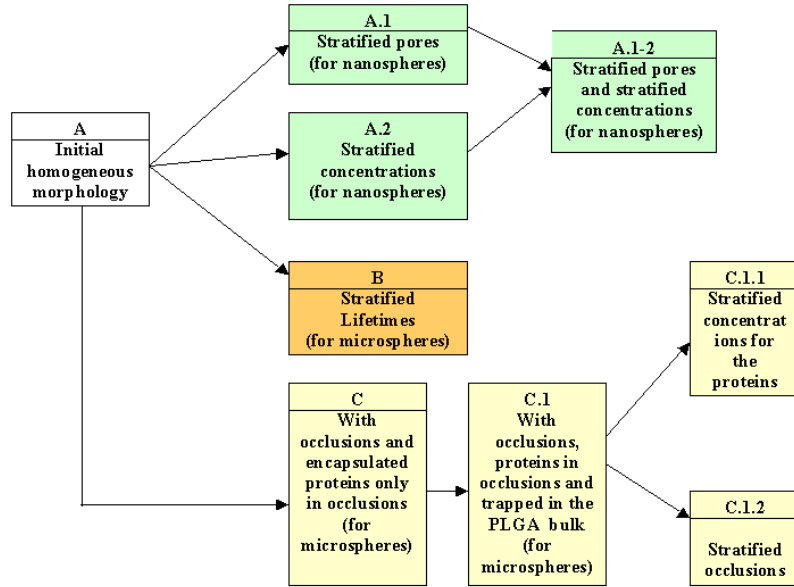
Fig. 6. Developmental scheme of the models and their variants.

Further, one should consider as well the possibility that PLGA might degrade quicker in the outer layers of the spheres than in the core. From gradient considerations, the degradation products have higher diffusivity in the mantle

of the sphere than in its core, thus the relative pore generation rate might increase more rapidly in the outer compared to the inner layers.

In this multi-agent investigation, these aspects were considered in an exploratory manner of increasing complexity. For example, the effects of a decreasing porosity from the surface to the core of the sphere, or of the protein adsorbed at the surface of the spheres, were considered by dividing a 3D sphere into strata and populating these with obstacles, pores and molecules according to different concentrations. Morphologies like those represented in Figure 2, (b), were directly taken into consideration by initialising a specific inner morphology containing both large occlusions filled with proteins and networks of smaller pores. Figure 6 shows the exploratory scheme of the variants for different inner morphologies of spheres spanning out of the initial model, (Figure 4).

For example, three different variants on the initial model A are presented, Figure 6. Version A.1 considers only stratified pores, with the porosities decreasing from the surface towards the centre. Version A.2 considers stratified concentrations of protein with similar gradient. However, it is reasonable to assume that layers with large initial porosities are correlated with correspondingly larger concentrations too, as described in [2, 21]. This is incorporated in version A.1-2. Other developments are also represented on the Figure 6 (models B and C and their variants).

4 Results and discussion

In the simulation, the number of particles per site was sampled from a uniform distribution between a lower and an upper value: $U(a1, a2), a1 < a2$. In this fine-grained simulation, the degrees of freedom, provided for the molecules by

the von Neumann neighbourhood (Figure 7, (a)), were sufficient to model the case. For coarser-grained models, e.g. cases where the molecules considered are much smaller then the site, a Moore's neighbourhood (Figure 7, (b)) can be considered, as offering more degrees of freedom. A broad sensitivity analysis has been carried out on the model, studying the effects on the dissolution profiles of parameters such as the erosion rate of the polymer, the distribution of proteins per site, the drug loading, the MC step time-interval (found to be a measure of the effective diffusivity of the protein), the type of neighbourhood used, the size of the sphere and the internal morphologies of the spheres. This section presents a discussion on a few of the most interesting aspects.
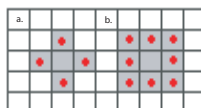

Fig. 7. a) Von Neumann neighbourhood in 2D. b) Moore's neighbourhood in 2D.

4.1 Initial porosity and initial macromolecular loading

Experimental work has shown that an increase in drug loading results in a corresponding increase in the release rate [15, 18]. Sandor et al. [18] have measured the protein loadings, as a percentage of the total weight of the nanospheres. Here it is considered in terms of the concentration of sites containing proteins. From the simulations, the loading value, i.e. concentration, appears to have no significant influence on the dissolution profiles, fact in accordance with parallel work [22] for release of protein from cross-linked polymers. Initially, this seems to be inconsistent with experiment, but [18] suggest that the increase in the release rate at higher loadings actually occurs due to *initial porosity*: at low loadings (0.5 -1.6 %), small proteins seem to

depend on diffusion through pores initially and on degradation at later times. Spheres with higher loadings are found to *have more interconnecting channels*. Sandor et al. [18] consider the channels to be the reason why the higher-loaded spheres (4.8-6.9 %) do not exhibit the pronounced shift (such as on Figure 8, filled circles) from diffusion-based (slow dissolution) to polymer release-based (higher dissolution rate) seen with the lower loaded spheres.
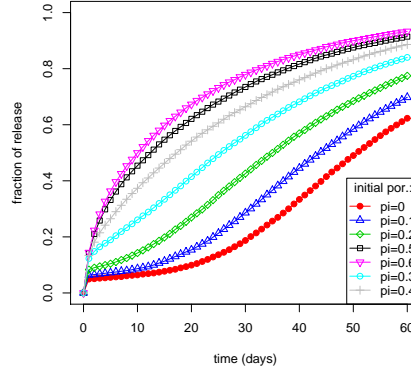
Fig. 8. Dissolution profile for different values of the initial porosity. Model inputs: d=100, λ=0.00001, Δt=10 min, c_0=0.02, from 1 to 4 particles per site, von Neumann neighbourhood.

Figure 8 shows the reaction to porosity variation in a sphere (d=100 and λ=0.00001), loaded with particles that are homogeneously distributed throughout its volume (c_0=0.02). As can be observed, even quite small variations of the initial porosity result in different dissolution profiles beginning with $\sim$ day 1 of dissolution.

In relation to the simulation, there is reason to believe that it is not variation in concentration, but rather *the variation of initial porosity*, which is the main basis for modification in dissolution profiles. There is a correlation of the dissolution profiles with the initial porosity resulting, in all probability, from

the way the spheres are manufactured. These simulations suggest that more attention should be dedicated to porosity studies in investigations on micro- and nanospheres, in order to better describe the connection between the concentration of the encapsulated molecule and the resulting initial porosity.

4.2 Influence of the MC time step

The physical meaning of the time interval Δt, during which the particles of the model move, is directly related to the mobility of the particles within the structure. The choice of Δt is determined by the effective diffusivity of a molecule in a medium filled with erosion products, such as different monomers. Smaller molecules have larger effective diffusivities, while larger molecules will be characterised by very reduced diffusivities [18]. Dimensional analysis has shown that in the cases of small to medium-sized proteins, Δt is of the order of seconds [1].

The spheres used in this simulation had porosity organised in 3 strata, with value decreasing from the mantle to the core. The simulation indicated more clearly the mechanisms behind the dissolution profiles. The smaller Δt is, the more frequently the particle may update, i.e. move to a neighbouring site with a specified probability. Figure 9, ($t>20$ days), shows that, in the case where the environment permits mobility, (right hand side of the graphs), different values for Δt can considerably change the rate of dissolution profile. The spheres started at zero initial porosity, but a small initial burst of particles released can still be observed. Further, the porosity was allowed to increase slowly, ($\lambda=0.00001$). At day 16, when the value of the porosity reached the threshold value of $p_{th}=0.2$, clusters of pores spanning the whole sphere started forming, hence the dissolution profiles begin to diverge according to the different values of Δt used.
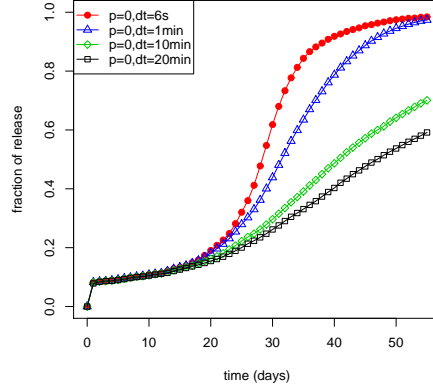
Fig. 9. Effect of the time step used to perform the updating in the simulation.

The fact that the problem is separable into two time domains - a fast domain representing the initial burst phase related to release of proteins from the pores connected to the outside, and a slow domain corresponding to formation of new connected pores by erosion - would actually permit an optimisation to the simulation. Simulating the initial phase with a very small Δt would permit to obtain more accurate representations of the burst phase.

4.3 Effect of internal morphology of the spheres

Figure 10 shows a comparison between the basic model A and its variants A.1 and A.1-2. Table 1 details the width of the strata, deliberately chosen in such a way that in each variant the initial porosity of the generated spheres was almost the same. Figure 10, (a) shows how the three variants behave with reduced initial porosity. Figures 10, (b) illustrate the behaviour of the three variants for a larger porosity. These results suggest that stratification of the porosity has a smaller role relative to the stratification of the molecule con-

centration. It also demonstrates that the internal morphology of the spheres is an important factor in modelling the micro- or nanosphere system.
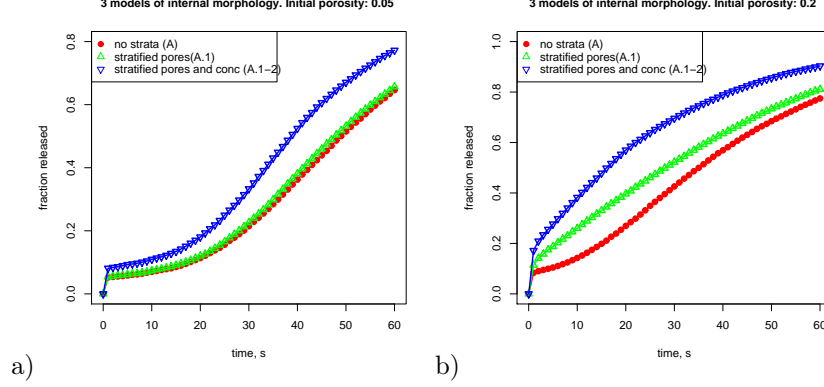

Fig. 10. Dissolution through spheres with homogeneous porosity (circles), spheres with stratified porosity (triangles) and combined stratified pores and stratified concentration (reversed triangles). a) $p_0 = 0.05$ b) $p_0 = 0.2$

4.4 Comparison with experimental data

To use the model and its variants for quantitative evaluations or predictions, initial specification of the microspheres is needed. Table 2 gives a list of parameters of the model. The values of these parameters have to be determined for *every* case to which the model is applied, because they are *directly* related to the internal structure and properties of the spheres. For the rest of this section, the results from the simulations are compared to real data.

4.5 Experimental Case 1: Lysozyme

In this subsection, the models are validated by comparing their performance to real data. The experimental data set from Sandor et al. [18] relates to a set of nanospheres encapsulating a very small protein, the lysozyme. Table 3 specifies the information available on this system.
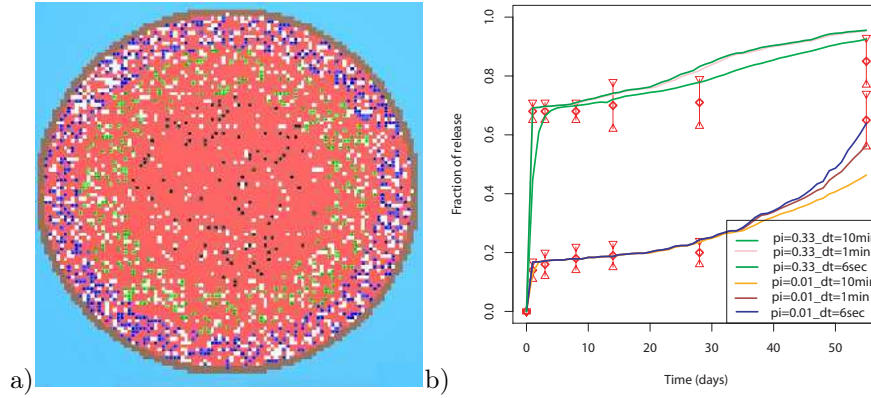
Fig. 11. a) Sphere with similar internal morphology to that used to model release of lysozyme. b) Experimental lyzosyme release versus simulated drug release from biodegradable microspheres. Rhombi represent the experimental points from [18]. Continuous curves show simulated results obtained with different Δt values.

The spheres have been analysed by electronic microscopy and they appear compact and non-porous [18]. This means that the pores, if these exist, have diameters < 20 nm i.e. below the resolution levels of the microscopy technique [18]. The existence of very small pores of 5 nm in diameter, (just above the Stokes-Einstein diameter of the lysozyme, 3 nm), has been assumed in the simulation. Given the diameter of the sphere d and the diameter of the pore p_d it was decided to run the simulations with spheres of 50 sites in diameter, (i.e. taking 5 nm as the diameter of one site). The λ parameter was chosen to be $5 \times 10^{-6} s^{-1}$ (corresponding to the erosion of the sphere in about 50 days). It was not known whether the pores were organised in strata or not, but, given that for slightly larger nanospheres, (encapsulating larger molecules, such as carbon anhydrase), porosities are known to be stratified [18], so it can be assumed here that spheres carrying lysozyme have stratified porosities as well. Models A, A1, A2 and A.1-2 have been tested for this system. Only model A.1-2 (model variant with stratified pores and stratified concentrations) has well replicated the experimental dissolution curves. Three different values

of $\triangle t$ have been chosen. The best results are obtained with the smallest time step: $\triangle t$=6 s, Figure 11, (b). Indeed, dimensional analysis has demonstrated that a $\triangle t$ of the order of seconds is a correct measure of the effective diffusivity of a protein in an eroding polymer medium [1]. In Figure 11, (b), the points indicating a slow release experimental curve correspond to an initial loading of 1.6% and the curve of very fast release has been obtained by Sandor et al. [18] with an initial loading of 6.9% of total weight.

4.6 Experimental Case 2: Carbonic Anhydrase

This subsection summarises results obtained with the model calibrated to simulate release of carbonic anhydrase from microspheres of size $\simeq 1$ μm, described, like previous spheres, in Sandor et al. [18]. This type of sphere has a very different initial internal morphology to the case examined previously. It is characterised by quite large internal pores and channels, which appear to be much larger then the protein diameter (carbon anhydrase). A model variant where initial pores were permitted to be larger in size than one site (C and variants) has been thus chosen. Figure 12, (a) shows a typical cross-section through a sphere generated with model C. In addition, most molecules are initially concentrated in these pores [2, 21]. In this model variant, most proteins are situated in the occlusions, but some are trapped in the bulk PLGA as well. The occlusions are slightly stratified, such that they are more prevalent at the surface of the spheres, replicating the pattern observed, Figure 5, (b). Table 4 shows the sphere data and modelling basis.

Figure 12, (b) illustrates the model's C.1.1 performance. The simulated slow release curve has been obtained with an initial porosity of 0.14 and the rapid release curve with initial porosity p_0=0.33. The experimental data were based on a population of spheres with average diameter of 1 μm. It should
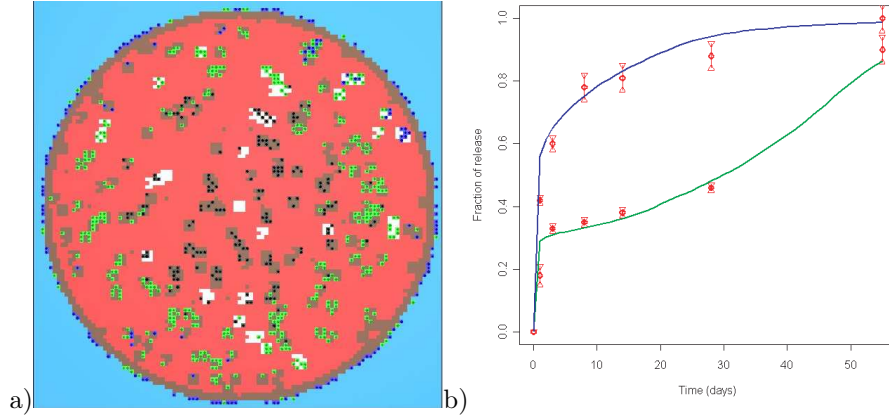
Fig. 12. a) Internal morphology of the spheres for simulating dissolution of carbonic anhydrase from PLGA spheres of $\simeq 1\mu m$ diameter. b) Experimental carbonic anhydrase versus simulated drug release from biodegradable microspheres. Red rhombi represent the experimental points from [18]. Continuous curves show simulated results obtained with different Δt values.

be noted that, in our experience, models variants which do not take into consideration the occlusions and the proteins trapped inside these, do not produce release profiles in agreement with known experimental dissolution profiles.

While microsphere internal structure is determined by the given experimental context, what the multi-agent approach actually does is provide a framework to allow us to determine those parameters based on emergent behaviour observed (or postulated) for the system, and not to rely on a complete knowledge of the *ab initio* conditions. The value of modelling work is that the framework, once developed, complements situations, where accurate experimentation is difficult, since it enables postulation of plausible system values and analysis of outcomes over a range. For example, in the case of nanospheres charged with lysozyme, the electronic microscopy was not sufficient to deter-

mine the inner structure of the spheres. Instead, we have made a range of assumptions about the internal morphology of the spheres, and several versions of the models where used to confirm or reject these assumptions, as described above.

5 Conclusions

The results of this multi-agent exploratory approach to modelling protein release from bioerodible PLGA spheres have demonstrated that Direct MC models can give very good quantitative agreement with experiment if enough consideration is given to the details (i.e. physical properties of spheres, parameter values,model variant etc). From the simulation technique point of view the major improvement in this work is the very fine-grained description of the systems, the close examination of the internal morphologies and the use of agents in the model building (for modelling the proteins). The models developed can be used in the optimisation process, by indicating what type of inner morphologies optimise the desired dissolution profile, and, in addition, for the inverse problem: assessment of the inner morphology of spheres based on the dissolution profiles, when microscopy data is not available.

References

[1] Barat, A. [2006], Probabilistic methods for drug dissolution, PhD thesis, Dublin City University.

[2] Batycky, R. P., Hanes, J., Langer, R. and Edwards, D. A. [1997], 'A theoretical model of erosion and macromolecular drug release from biodegrading microspheres ', *Journal of Pharmaceutical Sciences* (12), 1464–1477.

[3] Charlton, D., Peterson, M., Spiller, K., Lowman, A., Torzilli, P. and Maher, S. [2006], Mechanical Characterization of a Novel Scaffold for the Repair of Articular Cartilage . Private communication.

[4] Feng, S. [2006], 'Chemotherapeutic Engineering: Polymeric Nanoparticles for Clinical Administration of Anticancer Drugs '. Access date: 14/11/2006.

[5] Feng, S. and Chien, S. [2003], 'Chemotherapeutic engineering: application and further development of chemical engineering principles for chemotherapy of cancer and other diseases', *Chemical Engineering Science* **58**, 4087– 4114.

[6] Göpferich, A. [1995], 'Modeling of polymer erosion in three dimensions: rotationally symmetric devices', *American Institute of Chemical Engineers (AIChE) Journal* **41**(10).

[7] Göpferich, A. [1996], 'Mechanisms of polymer degradation and erosion', *Biomaterials* **17**, 103–114.

[8] Göpferich, A. [1997*a*], 'Bioerodible implants with programmable drug release', *Journal of Controlled Release* **44**, 271–281.

[9] Göpferich, A. [1997*b*], 'Erosion of composite polymer matrices', *Biomaterials* **18**, 397–403.

[10] Göpferich, A. and Langer, R. [1995], 'Modeling monomer release from bioerodible polymers', *Journal of Controlled Release* **33**, 55–69.

[11] Kang, F. and Singh, J. [2001], 'Effect of additives on the release of a model protein from PLGA microspheres ', *AAPS PharmSciTech* **2**(4), article 30.

[12] Kilic, A. C., Capan, Y., Vural, I., Gursoy, R. N., Dalkara, T., Cuine, A. and Hincal, A. A. [2005], 'Preparation and characterization of PLGA nanospheres for the targeted delivery of NR2B-specific antisense oligonu-

cleotides to the NMDA receptors in the brain ', *Journal of Microencapsulation* **22**(6), 633–641.

[13] Kisler, J. M., Stevens, G. W. and O'Connor, A. J. [2001], 'Adsorption of proteins on mesoporous molecular sieves', *Materials Physics and Mechanics* **4**, 89–93.

[14] Kosmidis, K., Rinaki, E., Argyrakis, P. and Macheras, P. [2003b], 'Analysis of case ii drug transport with radial and axial release from cylinders', *International Journal of Pharmaceutics* **254**.

[15] Lam, X., Duenas, E., Daugherty, A., Levin, N. and Cleland, J. [2000], 'Sustained release of recombinant human insulin-like growth factor-I for treatment of diabetes ', *Journal of Controlled Release* **67**, 281–292.

[16] Merkle, H., Gander, B., Meinel, L. and Walter, E. [2002], Novel Opportunities of Microparticulates for the Delivery of Therapeutics and Vaccines , Technical report.

[17] Nicholson, C. and Sychova, E. [1998], 'Extracellular space structure revealed by diffusion analysis', *Trends in Neurosciences* **21**(5), 207–215.

[18] Sandor, M., Enscore, D., Weston, P. and Mathiowitz, E. [2001], 'Effect of protein molecular weight on release from micron-sized PLGA microspheres', *Journal of Controlled Release* **76**, 297–311.

[19] Siepmann, J., Faisant, N. and Benoit, J.-P. [2002], ' A new mathematical model quantifying drug release from bioerodible microparticles using Monte Carlo simulations ', *Pharmaceutical Research* **19**(12), 1885–1893.

[20] ul Ain, Q., Sharma, S. and Khuller, G. K. [2003], 'Chemotherapeutic Potential of Orally Administered Poly(Lactide-Co-Glycolide) Microparticles Containing Isoniazid, Rifampin, and Pyrazinamide against Experimental Tuberculosis ', *Antimicrobial Agents and Chemotherapy* **47**(9), 3005–3007.

[21] Ungaro, F., Biondi, M., Indolfi, L., Rosa, G. D., Rotonda, M. I. L., Quaglia, F. and Netti, P. [2004], 'Bioactivated Polymer Scaffolds for Tissue Engineering ', *V Biomaterials* .

[22] Vlugt-Wensink, K. D., Vlugt, T. J., Jiskoot, W., Crommelin, D. J., Verrijk, R. and Hennink, W. E. [2006], 'Modeling the release of proteins from degrading crosslinked dextran microspheres using kinetic Monte Carlo simulations', *Journal of Controlled Release* **111**, 117–127.

[23] Zhang, M., Yang, Z., Chow, L.-L. and Wang, C.-H. [2003], 'Simulation of drug release from biodegradable polymeric microspheres with bulk and surface erosions ', *Journal of Pharmaceutical Sciences* **92**(10), 2040–2056.

[24] Zhao, A. and Rodgers, V. [2006], 'Using TEM to couple transient protein distribution and release for PLGA microparticles for potential use as vaccine delivery vehicles ', *Journal of Controlled Release* **113**(12), 15–22.

[25] Zygourakis, K. and Markenscoff, P. A. [1996], 'Computer-aided design of bioerodible devices with optimal release characteristics: a cellular automata approach', *Biomaterials* **17**, 125–135.

Table 1. Details on the stratification of the spheres used to obtain the results from Figure 10. r represents the radius of a sphere in number of sites, p_0 and c_0 are, respectively, the input porosity and concentration.

	Stratum1	Stratum2	Stratum3
Depth of stratum (sites)	$0.15r$	$0.25r$	$0.6r$
Porosity	$1.5p_0$	$0.7p_0$	$0.3p_0$
Concentration	$1.5c_0$	$0.7c_0$	$0.3c_0$

Table 2. Quantities needed for the simulation of protein dissolution from microspheres

Description	Variable
Size of the sphere	d
Effective diffusivity/mobility of the macromolecules through the pores	D_{eff}
Diffusivity of the macromolecules in the solvent	D_0
Diameter of the macromolecules	a
Sphere loading	c
Concentration of the macromolecule at different depths of the sphere	c_{01}, c_{02}, c_{03}
Size of the pore one wish to consider	p_d
Initial porosity	p_0
Pattern of repartition of pores in the volume of the sphere	p_{01}, p_{02}, p_{03}
Rate of pore formation	λ

Table 3. Properties of nanospheres loaded with lysozyme; corresponding modelling choices taken after evaluation of this data

Variable	Value	Model
d	200-250 nm	50 sites
D_{eff}	N/A	$\Delta t =$10min, 1min and 6 sec
D_0	N/A	not needed here
a	$\simeq$3 nm	-
c_0	1.6% and 6.9% of total weight	$c_{0low} =$0.016 and $c_{0high} =$0.069
$c_{01}/c_{02}/c_{03}$	N/A	$c_0/0.5c_0/0.2c_0$
p_d	>20 nm	5 nm/site
p_0	N/A	$p_{0low} =$0 and $p_{0high} =$0.3
$p_{01}/p_{02}/p_{03}$	N/A	$p_0/0.3p_0/0$
λ	N/A	5×10^{-6}

Table 4. Information available on nanospheres loaded with carbonic anhydrase; corresponding modelling decisions choses based on data evaluation

Variable	Value	Model
d	1000-1200 nm	100 sites
D_{eff}	N/A	$\Delta t =$1 min (by dimensional analysis)
D_0	N/A	not needed here
a	~10 nm	-
c_0	1.2% and 6%	$c_{0low} =$0.012 and $c_{0high} =$0.006
$c_{01}/c_{02}/c_{03}$	N/A	follows the occlusions
p_0	N/A	$p_{0low} =$0.14 and $p_{0high} =$0.33
$p_{01}/p_{02}/p_{03}$	N/A	2 strata: $r_1 = 5$, $r_2 = 45$ sites and $3p_0/p_0$
λ	N/A	5×10^{-6}